

# The influence of the disordered dipole subsystem on the thermal conductivity of the CO solid at low temperatures

V. Sumarokov

*B. Verkin Institute for Low Temperature Physics and Engineering of the National Academy of Sciences of Ukraine  
47 Lenin Ave., Kharkov 61103, Ukraine  
E-mail: sumarokov@ilt.kharkov.ua*

A. Jeżowski and P. Stachowiak

*W. Trzebiatowski Institute of Low Temperature and Structure Research of Polish Academy of Sciences  
P.O. Box 1410, 50-950 Wrocław, Poland  
E-mail: a.jezowski@int.pan.wroc.pl;  
p.stachowiak@int.pan.wroc.pl*

Received January 4, 2009

The thermal conductivity of solid CO was investigated in the temperature range 1–20 K. The experimental temperature dependence of thermal conductivity of solid CO was described using the time-relaxation method within the Debye model. The comparison of the experimental temperature dependences of the thermal conductivity of N<sub>2</sub> and CO shows that in the case of CO there is an additional large phonon scattering at temperatures near the maximum. The analysis of the experimental data indicates that this scattering is caused by the frozen disordered dipole subsystem similar to a dipole glass. The scattering is described by the resonant phonon scattering on tunnelling states and on low-energy quasi-harmonic oscillations within the soft potential model.

PACS: **63.20–e** Phonons in crystal lattices;  
**66.70.–f** Nonelectronic thermal conduction and heat-pulse propagation in solids; thermal waves;  
**44.10.+i** Heat conduction.

Keywords: thermal conductivity, heat transfer, molecular cryocrystals, dipolar disordered system.

## Introduction

Solid carbon monoxide (CO) belongs to a group of molecular cryocrystals with linear molecules, N<sub>2</sub> type crystals (N<sub>2</sub>, CO, CO<sub>2</sub>, and N<sub>2</sub>O) [1,2]. Solid CO was investigated in details by various methods: structural methods, Raman, IR spectroscopy, NQR and NMR methods, theoretical methods and others (see, e.g., Refs. 1–14). Heat capacity [15–21], thermal expansion [5,7,22,23] and propagation of sound [24] have been researched in details (see also parts 2 in books [1,2] and references therein).

Solid CO, being in equilibrium with its vapour, exists in two crystallographic phases. Under equilibrium vapour pressure, the structure of the low-temperature orientationally ordered  $\alpha$ -phase of carbon monoxide ( $T_{\alpha\beta} = 61.57$  K [19,25]) is the same as for  $\alpha$ -N<sub>2</sub> ( $T_{\alpha\beta} = 35.61$  K

[19,25]), namely, the fcc structure with an arrangement of molecular axes along the spatial diagonals of the elementary cell (the *Pa3* space group) [2] with four molecules in the cell. As the CO molecule has a nonzero permanent dipole moment, with decreasing temperature a dipole-ordering (ordering on the ends of molecules) and a phase transition into a lower temperature equilibrium phase of a structure *P2<sub>1</sub>3* (which differs from the *Pa3* structure mainly by that the CO molecules are ordered with respect to the ends) should occur. The theoretical estimation of temperature of such phase transition gives 5 K [26]. Although in the work by Vegard [3] the low-temperature structure of solid CO is determined as *P2<sub>1</sub>3*, researches on NQR [11,12], NMR [13], dielectric susceptibility [14], calorimetric [17,18,20,21], structural [5,6] studies specify that a non-equilibrium structure is observed. The au-

thors of the x-ray studies [5] concluded that in solid CO an «average»  $Pa3$  structure is observed, with the electron charge centres of the molecules localized in the lattice sites with the displaced mass centre of the molecule. Electron-diffraction results [6] and conclusions of lattice dynamics studies [10] are consistent with this conclusion. In the monograph on cryocrystals [2] (Chapter 12) the preference is also given to the structure with disordering with respect the ends of molecules. The estimation [12] of frequency ( $\sim 10^9 \text{ s}^{-1}$ ) of the end-to-end reorientations near the temperature of  $\alpha$ - $\beta$  phase transition (using NMR data [11]) testifies that the end-to-end ordering is practically absent in the high temperature region of  $\alpha$ -CO. The estimations [20,23] of the residual entropy of CO indicated that the majority of the CO molecules is in the disordered end-to-end reorientation state. Atake *et al.* [21] detected relaxation phenomena in the temperature drift in the temperature interval between 14 K and 19 K in low temperature calorimetric study of  $\alpha$ -CO, and concluded that the end-to-end reorientation freezes in this temperature interval, and defined the temperature of a transition to the glassy state ( $T_g \sim 18 \text{ K}$ ). However, this relaxation effect has not been observed in the thermal conductivity studies [27].

Since the disordered dipole subsystem of CO freezes, at low temperatures, local low-energy excitations, specific for glass-like systems, appear in the energy spectrum of the system. The phonon interaction with them should be reflected in the temperature dependence of the thermal conductivity.

The aim of this work is to investigate the influence of the disordered dipole subsystem on the heat transfer in CO solid at the low-temperature region of existence of  $\alpha$ -phase.

### Experiment

The studies of thermal conductivity of the solid CO were performed by the stationary method with the axial thermal flux [28] in the temperature range 1–20 K. Crystalline samples were grown directly in a measuring cylindrical glass cell of the dimensions: 67 mm in height, inner diameter of 6.4 mm and thickness of walls of 0.95 mm. Two germanium resistance thermometers, attached to the walls of the ampoule, were used for the measurement of temperature and temperature gradient. The distance between thermometers was equalled to 33 mm. The lower thermometer was on the distance about 14 mm from the bottom of the ampoule.

The samples were obtained from gas of 99.996 % purity. The gas had a natural isotope composition. CO crystals have been grown directly from the gaseous phase, passing the liquid phase, at the temperature slightly below the triple point. After growing and annealing of the sample at 59.5 K for 12 hours, the crystal was cooled down to

the temperature of liquid helium at the rate  $\sim 1 \text{ mm/h}$ . The time of passing of the  $\alpha$ - $\beta$  phase transition was about 70 h.

The random error of low-temperature measurements did not exceed 1.5%. The other details of the experiment were described in Ref. 27.

### Results and discussion

The thermal conductivity of  $\alpha$ -CO has been investigated in the temperature interval 1–20 K. Previous experimental results are presented in Ref. 27. The experimental temperature dependence of the thermal conductivity  $\kappa(T)$  of CO is shown in Fig. 1. The behavior of  $\kappa(T)$  qualitatively is typical for dielectric crystals. The thermal conductivity increases with temperature, reaching a maximal value 28 mW/(cm·K) at  $T_{\text{max}} \approx 6 \text{ K}$ . For comparison, in the same Figure the experimental curve of the thermal conductivity of nitrogen [29] is also shown.

Solid carbon monoxide and nitrogen have much in common, and in many aspects solid CO is an analogue of  $\text{N}_2$ . They have close molecular and crystal parameters [1,2] (molecular mass, lattice parameter, structure of both

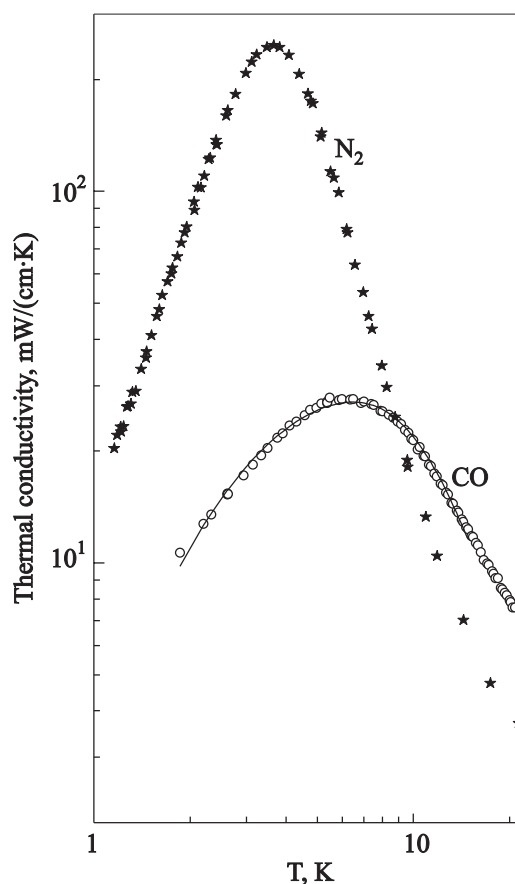


Fig. 1. Low-temperature thermal conductivity of crystalline CO and  $\text{N}_2$ . Experiment (O) — CO, (★) —  $\text{N}_2$  from Ref. 29. Fitting: solid line — CO according Eq. (5).

solid-state phases, etc.). As a result, one could expect that experimental curves of thermal conductivity for both crystals should be close to each other. However, like in the case of CO<sub>2</sub> and N<sub>2</sub>O [30], low temperature thermal conductivities of CO and N<sub>2</sub> differ appreciably. In the high temperature region thermal conductivity of CO is much higher than that of nitrogen. For example, thermal conductivity of carbon monoxide at 20 K is twice as large as that of nitrogen. However, with decreasing temperature the character of temperature dependence of thermal conductivity of CO changes sharply and the CO curve crosses the nitrogen curve near 9 K. The maximum of the temperature dependence of thermal conductivity for carbon monoxide is an order of magnitude lower than that of nitrogen, and is shifted to a higher temperature region. The maxima differ considerably in the shape, being much broader for CO than N<sub>2</sub>. The comparison of their temperature dependences shows that in the case of carbon monoxide there is an additional large scattering of phonons in comparison with nitrogen.

Recently, it was found out that the influence of the disordered dipole subsystem on the heat transfer in solid N<sub>2</sub>O in the low temperature region results in the large reduction of thermal conductivity of N<sub>2</sub>O in comparison with CO<sub>2</sub> [30]. In Ref. 30 this large reduction was explained within the framework of the model of soft potentials (SPM) [31] as being the result of the resonant phonon scattering at the tunnel two-level systems and low-energy soft quasi-harmonic oscillations.

The principal difference between CO and N<sub>2</sub> lies in the fact that the CO molecule has a non-zero permanent dipole moment. Since the disordered dipole subsystem of CO is frozen at low temperatures, there are local low-energy excitations specific for glass-like systems. The phonon interaction with them is reflected in the temperature dependence of the thermal conductivity.

Experimental results were analyzed using the time-relaxation method [28] within the Debye model. The thermal conductivity of dielectric solids can be written in the form

$$\kappa = GT^3 \int_0^{\Theta/T} \tau_R f(x) dx, \quad (1)$$

where  $G = k_B^4 / 2\pi^2 v \hbar^3$ ,  $f(x) = x^4 e^x / (e^x - 1)^2$ ,  $x = \hbar\omega / k_B T$ ,  $k_B$  is the Boltzmann constant,  $\hbar$  is the Planck constant,  $\omega$  is the phonon frequency,  $\Theta$  is the characteristic Debye temperature,  $\tau_R$  is the relaxation time for the «resistive» interaction processes,  $v = [(v_l^{-3} + 2v_t^{-3})/3]^{-1/3}$  is the sound velocity averaged over the longitudinal  $v_l$  and transverse  $v_t$  polarizations [28].

Experimental results of thermal conductivity were analyzed disregarding both the contribution of the librions to the heat transfer and the phonon scattering by librations,

since the lowest libron excitation level is about 44.5 cm<sup>-1</sup> (65 K) [2].

Assuming that different scattering mechanisms are independent, the relaxation time  $\tau_R$  can be written as

$$\tau_R^{-1} = \sum \tau_i^{-1}. \quad (2)$$

Here  $\tau_i^{-1}$  ( $i = b, p, d, u$ ) are the relaxation rates in different mechanisms of the phonon scattering processes. The temperature and frequency dependences of the relaxation rates [28] for the phonon scattering on the grain boundaries, stress fields of dislocations, isotopic impurities and in the U-processes are as follows:

$$\begin{aligned} \tau_b^{-1} &= a_b; \quad \tau_d^{-1} = a_d x T; \quad \tau_p^{-1} = a_p x^4 T^4; \\ \tau_u^{-1} &= a_{1u} x^2 T^5 \exp(-a_{2u} / T). \end{aligned} \quad (3)$$

The obtained experimental data were approximated using our procedure described in Ref. 29. The parameters  $a_j$  ( $j = b, p, d, 1u, 2u$ ) were estimated by minimizing the functional  $\sum [(\kappa_{ci} - \kappa_{ei}) / \kappa_{ei}]^2$ , where  $\kappa_{ci}$  and  $\kappa_{ei}$  are the calculated and experimental thermal conductivity coefficients, respectively, at the  $i$  th point. The calculation was performed using the values from Ref. 2:  $\Theta = 103$  K,  $v_l = 2014.5$  m/s,  $v_t = 1103.5$  m/s.

An approximation of the experimental temperature dependence of thermal conductivity of carbon monoxide fails to be described in the low temperature region by Eq. (1) taking into account Eqs. (2) and (3).

To account for the extra (in comparison with N<sub>2</sub>) large phonon scattering in solid CO it is necessary to introduce an additional summand into the expression for the relaxation time  $\tau_R^{-1}$  (2), as it was done in the case of N<sub>2</sub>O [30]. We described this additional scattering mechanism in the model of soft potentials [31]. The expression for the relaxation rate  $\tau_{sp}^{-1}$  of acoustic phonons can be written as follows:

$$\tau_{sp}^{-1} = c_1 x T \tanh \frac{x}{2} + c_2 (xT)^4 + c_3 x T^3. \quad (4)$$

The first summand describes the resonant scattering of phonons on the tunnel states (TLS), the second and the third terms describe the scattering on low-energy soft quasi-harmonic oscillators [31].

The fitting procedure gives the combined relaxation time:

$$\begin{aligned} \tau_R^{-1} &= 2.86 \cdot 10^7 + 12.9 x^4 T^4 + 2.41 \cdot 10^5 x T + \\ &+ 1.77 \cdot 10^4 x^2 T^5 \exp(-12.55 / T) + 2.63 \cdot 10^7 x T \tanh \frac{x}{2} + \\ &+ 25.8 (xT)^4 + 3.07 \cdot 10^6 x T^3. \end{aligned} \quad (5)$$

Figure 1 shows the fitting curve (solid line) describing the thermal conductivity of solid CO. It can be seen that below 17 K the description of the experimental results is

quite good. On this ground, we concluded that the influence of the disorder dipole subsystem on thermal conductivity of crystal CO can be described within the framework of the SPM model.

Using the obtained values (5) of the intensity of the phonon scattering and Eq. (3) for relaxation times we estimated [28] the crystallite size, density of dislocations,

and density of isotope defects. The size of crystalline grains,  $4.3 \cdot 10^{-2}$  mm, is close to that for nitrogen. The density of dislocations,  $4.3 \cdot 10^8$  cm<sup>-2</sup>, in CO is smaller than in N<sub>2</sub>. The intensity of the phonon–phonon interaction in solid CO is six times less than in N<sub>2</sub>.

Figure 2 shows the relaxation rates of phonons versus phonon energy for different temperatures from 1.5 K up

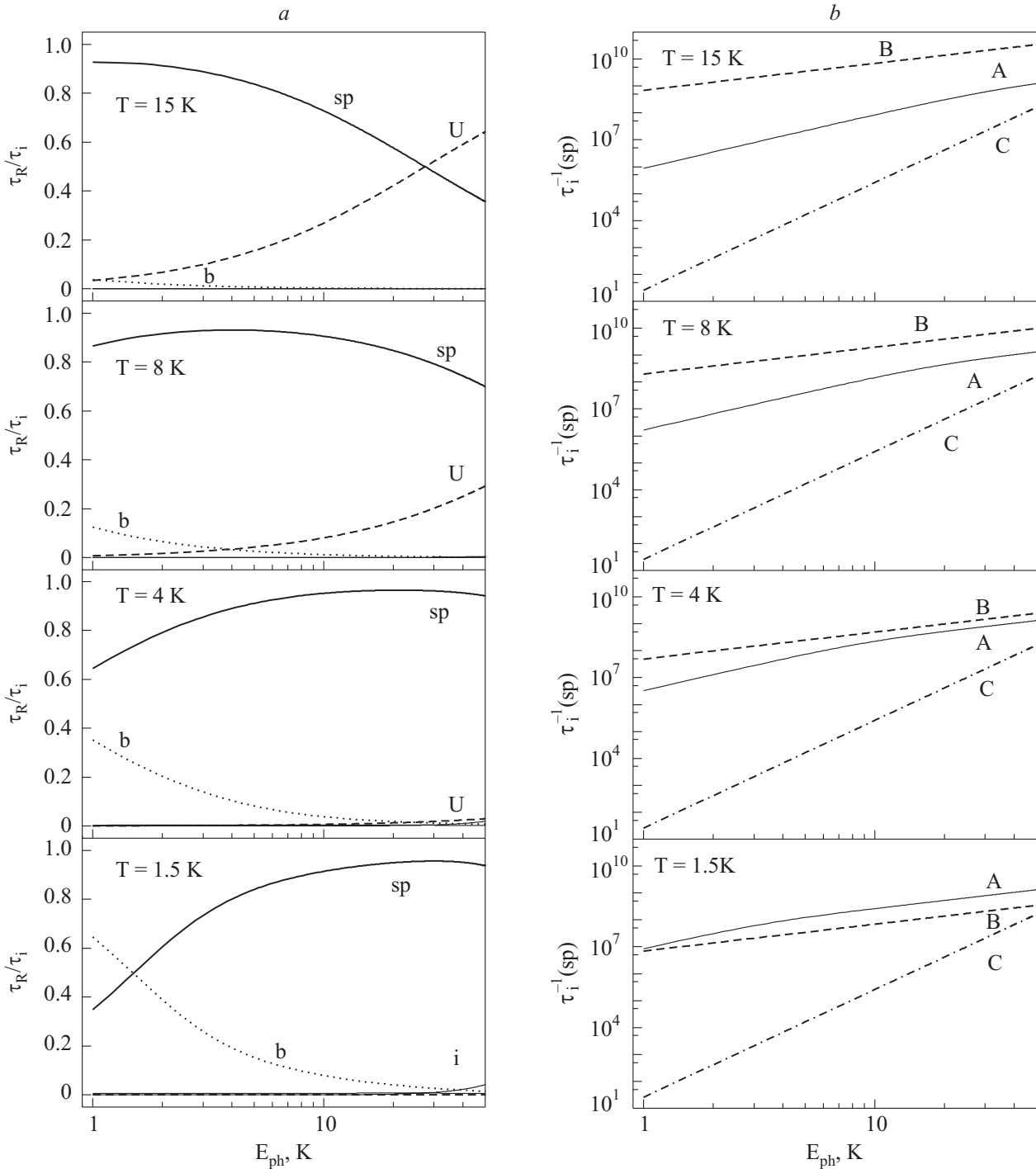


Fig. 2. Ratio of the relaxation rate for the individual scattering processes  $\tau_i^{-1}$  ( $i = b, d, i, u, sp$ ) to the «resistive» relaxation rate  $\tau_r^{-1}$  versus the phonon energy. Scattering of phonons:  $b$  — on grain boundaries,  $d$  — on dislocation stress fields,  $i$  — on point defects,  $u$  — on phonons (the  $U$ -processes),  $sp$  — the resonant phonon scattering on tunnel states and on low-energy vibrations with the framework of the model of soft potentials (a). The relaxation rate for the individual scattering processes  $\tau_{isp}^{-1}$  ( $i = A, B, C$ ) versus the phonon energy. The resonant phonon scattering: on tunnel states (A) and on low-energy quasi-harmonic oscillations (B, C) (b).

to 15 K. The ratio of the relaxation rate of the individual scattering processes  $\tau_i^{-1}$  ( $i = b, d, i, u, sp$ ) to the «resistive» relaxation rate  $\tau_R^{-1}$  versus the phonon energy is depicted in Fig. 2,a. The contribution of the boundary scattering is essential at 1.5 K for low-energy phonons and tends to decrease with increasing temperature. The  $\tau_{sp}^{-1}$  is the main contribution at temperatures 1.5–15 K, it is the second largest exceeded only by the boundary scattering for low-energy phonons below 1.5 K, and above 15 K it is the second largest exceeded by the contribution from U-processes for phonons with energy over 25 K. Contributions of other scattering mechanisms are negligible.

Figure 2,b shows the relaxation rate for the individual scattering processes  $\tau_{isp}^{-1}$  ( $i = A, B, C$ ) as a function of the phonon energy (see (4)), where  $A, B,$  and  $C$  are the resonant phonon scattering on the tunnel states  $A$ , and low-energy quasi-harmonic oscillators  $B$  and  $C$ . The relaxation rate  $A$  from TLS is close to the relaxation rate  $B$  from the second summand at 1.5 K. When temperature increases the relaxation rate  $B$  becomes dominant in comparison with the rates  $A$  and  $C$ . The relaxation rate  $C$  is smaller than others by the several orders of magnitude.

The resonant phonon scattering on quasi-local elementary excitations not only makes possible to describe the thermal conductivity  $k(T)$  of solid CO, but also allows to explain the large difference in the thermal conductivity of solid CO and  $N_2$  in the low temperature region. To this end we shall replace  $\tau_R^{-1}(N_2)$ , allowing to describe  $k(T)$  for  $N_2$  (curve 1, Fig. 3), by  $\tau_R^{-1}(N_2) \Rightarrow \tau_R^{-1}(N_2) + \tau_{sp}^{-1}(CO)$ . As a result we received the curve 2 (Fig. 3), which describes well the thermal conductivity of solid CO below the maximum point. The curve 2 transforms into the curve 3, taking into account distinctions in the parameters of U-processes.

Thus, the relaxation time  $\tau_{sp}^{-1}$  (4) allows to describe both the temperature dependence of the thermal conductivity of CO, and the large difference in thermal conductivities of solid CO and  $N_2$  at low temperatures.

### Conclusions

The thermal conductivity of solid CO was studied in the temperature range 1–20 K. The experimental temperature dependence of the thermal conductivity of solid CO was described using the time-relaxation method within the Debye model. Analysis shows that for solid CO the following can be stated: the size of crystalline grains is close to that of nitrogen, the density of dislocations is smaller than in nitrogen, and the intensity of the phonon–phonon interaction is six times less than in nitrogen.

The comparison of the experimental temperature dependences of the thermal conductivity of solid  $N_2$  and CO shows that in the case of CO there is an additional large phonon scattering at temperatures near the maximum. The analysis of the experimental data indicates that this

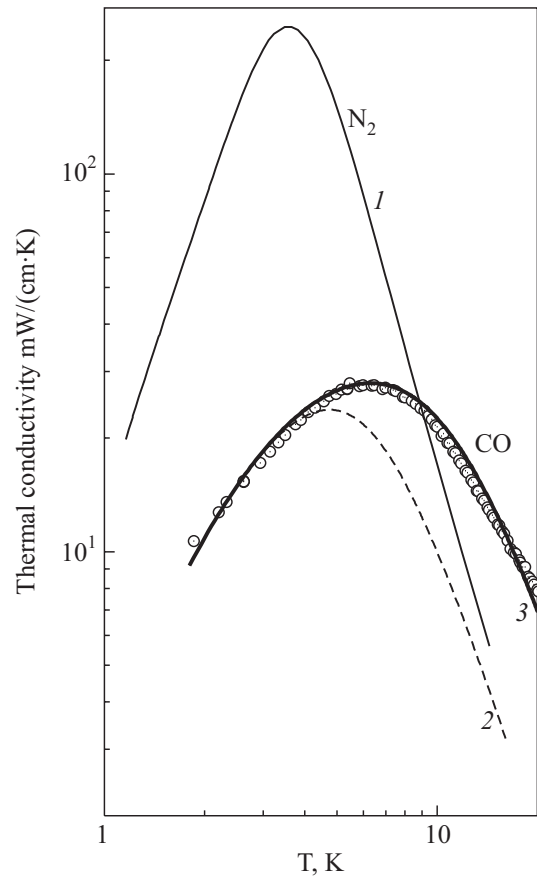


Fig. 3. The temperature dependence of thermal conductivity. Experiment: circles — CO, curve 1 —  $N_2$ . The curves 2 and 3 are described in the text.

scattering is caused by the frozen disordered dipole subsystem similar to the dipole glass. This scattering is described by the resonant phonon scattering on tunnelling states and on low-energy quasi-harmonic oscillations within the soft potential model.

The authors gratefully thank Yu.A. Freiman for fruitful discussion.

1. Kriocrystally, B.I. Verkin and A.F. Prichotko (eds.), Naukova Dumka, Kiev (1983).
2. *Physics of Cryocrystals*, V.G. Manzhelii and Yu.A. Freiman (eds.) AIP, NY (1997).
3. L. Vegard, *Z. Phys.* **61**, 185 (1930).
4. L. Vegard, *Z. Phys.* **88**, 235 (1934).
5. I.N. Krupskii, A.I. Prokhvatilov, A.I. Erenburg, and L.D. Yantsevich, *Phys. Status Solidi (a)* **19**, 519 (1973).
6. S.I. Kovalenko, E.I. Indan, A.A. Khudotyoplyaya, and I.N. Krupskii, *Phys. Status Solidi (a)* **20**, 629 (1973).
7. I.N. Krupskii, A.I. Prokhvatilov, A.I. Erenburg, and A.P. Isakina, *Fiz. Nizk. Temp.* **1**, 726 (1975) [*Sov. J. Low Temp. Phys.* **1**, 550 (1975)].
8. A. Anderson, T.S. Sun, and M.C.A. Donkersloot, *Can. J. Phys.* **48**, 2265 (1970).



9. M. Vetter, A.P. Brodyanski, S.A. Medvedev, and H.J. Jodl, *Phys. Rev.* **B75**, 014305 (2007).
10. W.B.J.M. Janssen, J. Michiels, and A. van der Avoird, *J. Chem. Phys.* **94**, 8402 (1991).
11. F. Li, J.R. Brookeman, A. Rigamonti, and T.A. Scott, *J. Chem. Phys.* **74**, 3120 (1981).
12. J. Walton, L. Brookeman, and A. Rigamonti, *Phys. Rev.* **B28**, 4050 (1983).
13. S.-B. Liu, and M.S. Conradi, *Phys. Rev.* **B30**, 24 (1984).
14. K.R. Nary, P.L. Kuhns, and M.S. Conradi, *Phys. Rev.* **B26**, 3370 (1982).
15. A. Eucken, *Vert. Deutsch. Physikal. Ges.* **18**, 4 (1916).
16. K.Z. Clusius, *Phys. Chem.* **B3**, 41 (1929).
17. J.O. Clayton and W.F. Giaque, *J. Am. Chem. Soc.* **54**, 2610 (1932).
18. E.K. Gill and L.A. Morrison, *J. Chem. Phys.* **45**, 1585 (1966).
19. T. Shinoda, T. Atake, H. Chihara, Y. Mashiko, S. Seki, and Kogyo Kagaku Zasshi, *J. Chem.Soc. Jpn. Industr. Chem. Sec. 3* **69**, 1619 (1966).
20. J.C. Burford and C.M. Graham, *Can. J. Phys.* **47**, 23 (1969).
21. T. Atake, H. Suga, and H. Chihara, *Chem. Lett.* **5**, 567 (1976).
22. E.I. Voitovich, A.M. Tolkachev, V.G. Manzhelii, and V.G. Gavrilko, *Ukr. Fiz. Zh.* **15**, 1217 (1971).
23. A.M. Tolkachev, V.G. Manzhelii, V.P. Azarenkov, A. Jeżowski, and E.A. Kosobutskaya, *Fiz. Nizk. Temp.* **6**, 942 (1980) [*Sov. J. Low Temp. Phys.* **6**, 747 (1980)].
24. P.A. Bezuglyi, L.M. Tarasenko and Yu.S. Ivanov, *Fiz. Tverd. Tela* **10**, 2119 (1968).
25. E. Fukushima, A.A.V. Gibson, and T.A. Scott, *J. Low Temp. Phys.* **28**, 157 (1977).
26. M.W. Melhuish and R.L. Scott, *J. Phys. Chem.* **68**, 2301 (1964).
27. P. Stachowiak, V.V. Sumarokov, J. Mucha, and A. Jeżowski, *J. Low Temp. Phys.* **111**, 379 (1998).
28. R. Berman, *Thermal Conduction in Solids*, Clarendon, Oxford (1976).
29. P. Stachowiak, V.V. Sumarokov, J. Mucha, and A. Jeżowski, *Phys. Rev.* **B50**, 543 (1994).
30. V.V. Sumarokov, P. Stachowiak, and A. Jeżowski, *Fiz. Nizk. Temp.* **33**, 778 (2007) [*Low Temp. Phys.* **33**, 595 (2007)].
31. D.A. Parshin, *Fiz. Tverd. Tela* **36**, 1809 (1994).